

# Mechanical Properties in the Ceria–Zirconia System

S. Maschio, O. Sbaizero & S. Meriani

Istituto di Chimica Applicata ed Industriale, Via A. Valerio 2, University of Trieste, I-34127 Trieste, Italy

(Received 28 February 1991; revised version received 10 July 1991; accepted 22 July 1991)

## Abstract

*The room temperature mechanical properties of samples ranging through the whole zirconia–ceria system have been determined and related to the phases present in order to establish the influence of crystallographic parameters on the material properties. Hardness, toughness and strength as a function of the amount of transformable tetragonal, non-transformable tetragonal or cubic zirconia are discussed.*

*Im gesamten binären System  $\text{ZrO}_2$ – $\text{CeO}_2$  wurden die mechanischen Eigenschaften bei Raumtemperatur gemessen und mit den jeweils vorherrschenden Phasen korreliert, um den Einfluß der kristallographischen Parameter auf die Materialeigenschaften zu bestimmen. Die Abhängigkeit der Härte, Zähigkeit und Festigkeit vom Anteil an umwandlungsfähigem tetragonalem  $\text{ZrO}_2$ , nicht umwandlungsfähigem tetragonalem  $\text{ZrO}_2$  oder kubischem  $\text{ZrO}_2$  wird diskutiert.*

*Les propriétés mécaniques, à température ambiante, d'échantillons balayant, en composition, tout le système zircone–oxyde de cérium ont été mesurées, puis mises en relation avec les phases présentes, dans le but d'établir l'influence des paramètres cristallographiques sur les propriétés du matériau. On discute de la dureté, de la ténacité et de la résistance, en fonction des quantités en zircone tétragonale transformable, zircone tétragonale non-transformable ou zircone cubique.*

## 1 Introduction

The ceria–zirconia system is being developed as an alternative to the more investigated yttria–zirconia

because of its better thermal stability in a moist environment<sup>1</sup> and the wider region where stabilisation of tetragonal  $\text{ZrO}_2$  is possible.<sup>2</sup> Furthermore, the system is interesting for the presence of two tetragonal phases:<sup>3–4</sup> one, usually called  $\text{TZ}^0$ , is the one stable for  $\text{CeO}_2$  compositions ranging from 7.5 to 16 mol%; the other one, here called  $\text{TZ}'$ , exists for compositions from 16 to 50 mol%. The former can transform under an applied stress raising the material toughness; the latter cannot transform as it derives from the high temperature cubic form (CZ), through an appropriate cooling rate, which re-equilibrates the oxygen content, resulting in a displacive transformation to a high ceria content tetragonal phase. For  $\text{CeO}_2$  less than 7.5 mol% the only phase present is monoclinic while for  $\text{CeO}_2$  content above 50 mol% it is cubic.

Despite extensive investigations on the mechanical properties of these materials, previous work has concentrated on compositions ranging from 10 to 16 mol%  $\text{CeO}_2$ .<sup>5–7</sup> Therefore only partial information on the relative influence of these two tetragonal phases is available.

Unfortunately  $\text{CeO}_2$ – $\text{ZrO}_2$  solid solutions show limited sinterability and even methods like hot or hot-isostatic pressing are not suitable, since  $\text{Ce}^{4+}$  readily reduce to  $\text{Ce}^{3+}$  during the process and this enhances the tetragonal (*t*) to monoclinic (*m*) transformation during cooling,<sup>1</sup> degrading the overall mechanical properties.

For low  $\text{CeO}_2$  alloys (below 16 mol%) high density may be achieved with a sintering temperature ranging from 1400 to 1450°C.<sup>2</sup> Above 1450°C cerium oxide occurs in its reduced form,  $\text{Ce}_2\text{O}_3$ , and Heussner and Claussen<sup>8</sup> have pointed out that such  $\text{ZrO}_2$ – $\text{Ce}_2\text{O}_3$  solid solutions are monoclinic at room temperature. Therefore long sintering times as well as high sintering temperatures favour the presence

of the *m*-phase in the sample core. This fact, together with the formation of large grains, is responsible for the microcracks which adversely affect the material's final density and the mechanical properties.

Samples with CeO<sub>2</sub> content above 50 mol% at the aforementioned temperatures do not reach good density and sintering temperatures close to 1600°C are required. For these reasons we have chosen to sinter all samples in the present work at 1600°C.

The aim of the research has been to correlate hardness, strength and toughness with the CeO<sub>2</sub> content, and with the microstructures and phases present.

## 2 Experimental

Samples of composition ranging through the whole zirconia–ceria system were prepared by ball milling CeO<sub>2</sub> (Medolla) and ZrO<sub>2</sub> (TZO Tosoh) in the appropriate proportions. Mixtures were pressed at 110 MPa to form cylinders and bars to be fired at 10°C/min up to 1600°C and soaked for 2 h.

Phases were identified by their X-ray diffraction (XRD) pattern, recorded directly from the pellet's surface with CuK<sub>α</sub> (Ni filtered) radiation on a powder diffractometer (Siemens Compensograph).

Densities were measured on fired specimens by the water displacement method whereas theoretical values were calculated by applying crystallographic data for ceria–zirconia solid solutions.<sup>4</sup>

Sample surfaces were polished down to 3 μm by diamond paste, the samples being then annealed for 30 min at 1400°C to recover any stress-induced phase transformation.

Hardness was measured by the Vickers indentation procedure following the recommendations of Anstis *et al.*<sup>9</sup> Loads ranging from 50 to 20 N were used to measure the whole series. The lower loads were needed to test samples with higher ceria concentration to avoid crack formation and propagation from the indentation marks. Reported hardness data reflect a mean value of 10 indentations.

Strength was evaluated in the four-point bend test (10 mm inner, 30 mm outer spans) using a crosshead speed of 0.05 mm/min.

Toughness was measured following the single edge notch beam (SENB) technique.<sup>10,11</sup> Notches were made with a 100-μm cutting wheel and specimens were broken using the strength evaluation procedure.

Microstructures of polished and thermally etched surfaces were examined with a scanning electron microscope.

## 3 Results and Discussion

The sintering experiments were carried out at 1600°C with holding times from 0 to 10 h. Figure 1 shows the relative density as a function of sintering time. For compositions above 32 mol% CeO<sub>2</sub> density increases with sintering time, but after 2 h nearly 99% of the final density is already reached. For compositions below 32 mol% the maximum density is reached after 2 h and then it slightly decreases. For longer sintering time the density decreases owing to microcracks associated with the growing grain size and the ensuing *t*–*m* transformation.<sup>1</sup>

The microstructure development during sintering was further investigated by SEM analysis. An SEM micrograph of the polished and thermally etched surface is given in Fig. 2; it shows ZrO<sub>2</sub>–CeO<sub>2</sub> 16 mol% after 2 h at 1600°C, where only the tetragonal TZ<sup>0</sup> phase is present. Microstructures are similar for all compositions and differences in average grain size as a function of composition are very limited, and remain comparable even when the CeO<sub>2</sub> is increased up to 90 mol%. The average grain size is 3.5 μm, larger than that reported in Refs 5 and 6. Resultant mechanical properties should then be less favourable but the overall behaviour should not change.

The phase composition derived by XRD (Table 1) is in good agreement with previous studies,<sup>12</sup> except for the sample with 10 mol% of CeO<sub>2</sub>, where some monoclinic phase was detected probably because of the grain size.

In Figs 3 and 4 strength and toughness as a function of ceria content are reported. As expected,<sup>2</sup>

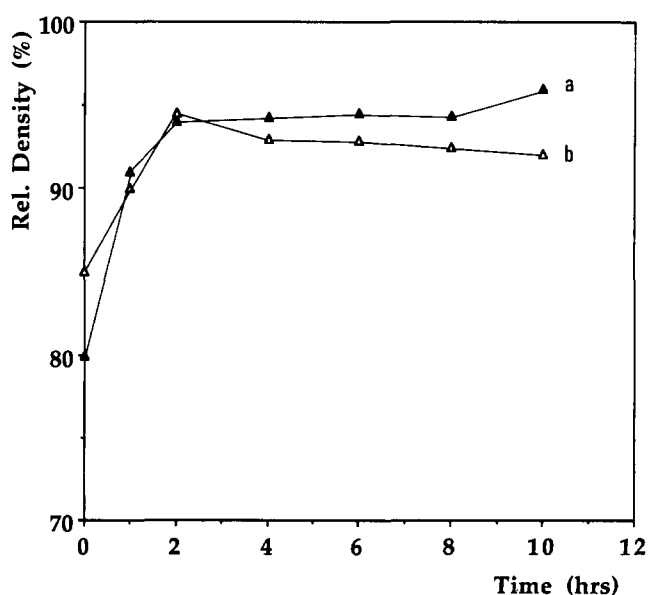


Fig. 1. Relative density versus sintering time for two samples with different CeO<sub>2</sub> content: (a) 48 mol% and (b) 24 mol%.

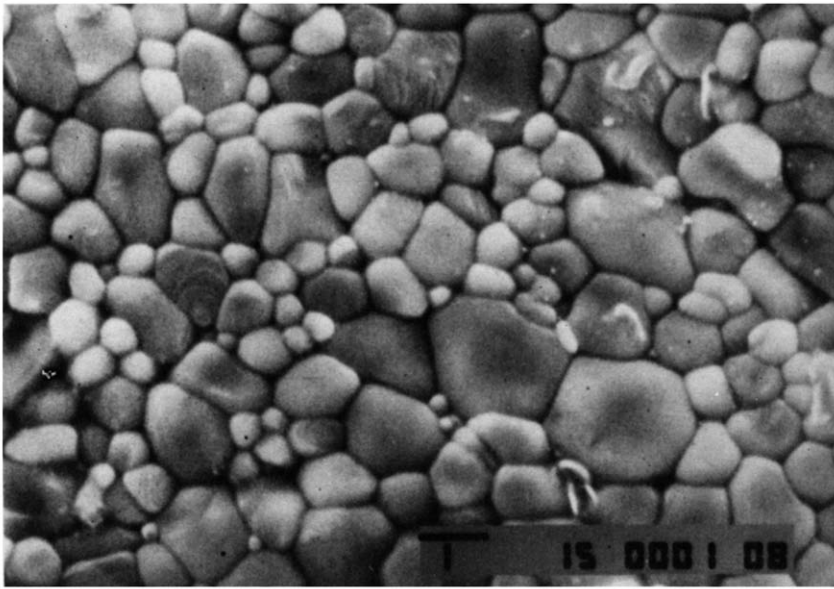


Fig. 2. SEM microstructure of a polished and thermally etched surface of a  $\text{ZrO}_2$ - $\text{CeO}_2$  24 mol% sample.

Table 1. Physical properties of tested samples (sintered at  $1600^\circ\text{C}$  for 2 h)

$\text{CeO}_2$ (mol%)	Phases	% Theoretical density
10	$m + \text{TZ}^0$	94.5
12	$\text{TZ}^0$	94.5
14	$\text{TZ}^0$	94
16	$\text{TZ}^0$	95
24	$\text{TZ}^0 + \text{TZ}'$ ( $\text{TZ}^0 \sim 70\%$ )	96
32	$\text{TZ}' + \text{TZ}^0$ ( $\text{TZ}^0 \sim 30\%$ )	95.5
40	$\text{TZ}'$	96
48	$\text{TZ}'$	95
60	Cub	95.5
70	Cub	94.5
80	Cub	94.5
90	Cub	96
100	Cub	94

both values show a sharp peak at about 12–14 mol%, which coincides with the marked decrease of  $m\text{-ZrO}_2$  and the appearance of the  $\text{TZ}^0$  phase. Further addition of ceria results in a decrease of both strength and toughness. This decrease can be divided into two regions: the first up to 48 mol% of  $\text{CeO}_2$ , where both fall very steeply; the other beyond 50 mol%, where there is a gradual decrease in toughness whereas strength remains almost constant.

The trend may be explained by the fact that in the 12–14 mol% material the majority of the sample is the  $\text{TZ}^0$  phase, which gives rise to transformation toughening, able to absorb energy when the fracture propagates. As the amount of ceria increases, strength as well as toughness decreases, since the  $\text{TZ}'$  phase is ineffective for improving toughness.

It is worth pointing out that compositions up to

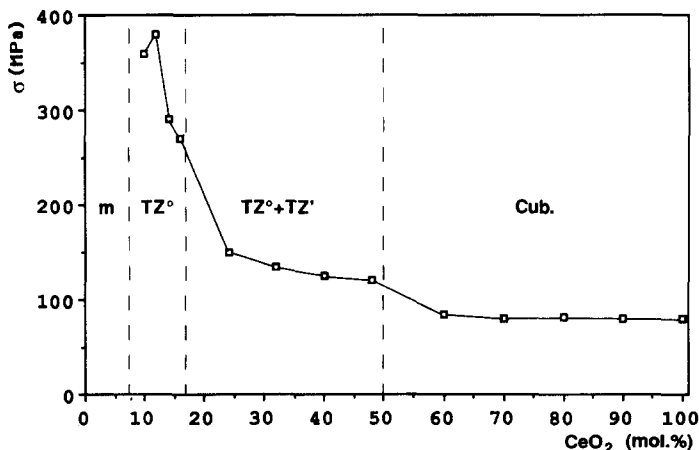


Fig. 3. Bend strength versus  $\text{CeO}_2$  mol% assessed using the four-point bend test.

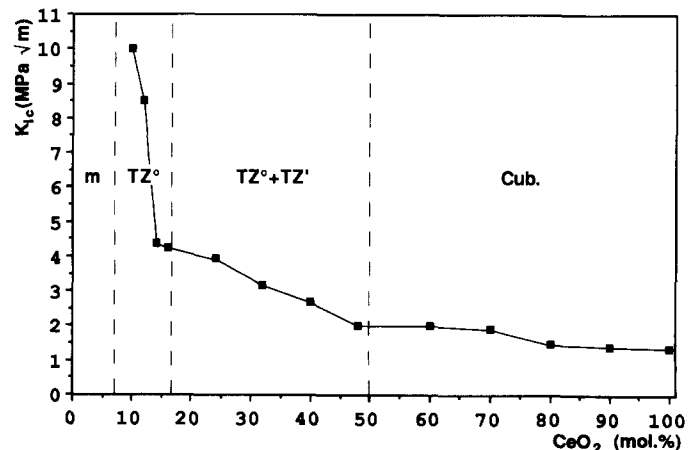


Fig. 4.  $K_{1c}$  versus  $\text{CeO}_2$  content measured by the notch-beam technique.

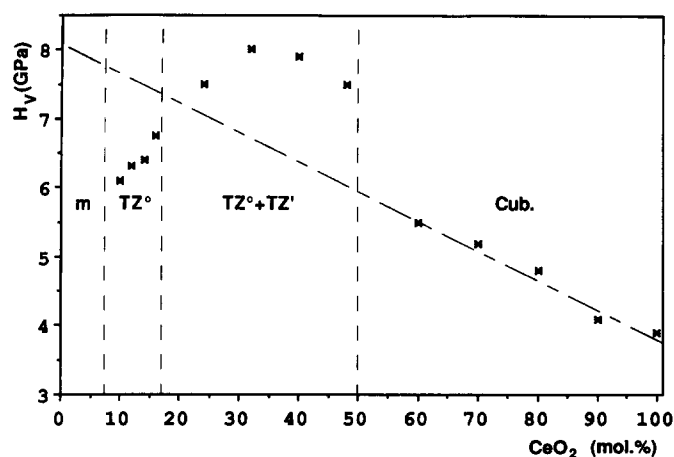


Fig. 5. Vickers hardness versus CeO<sub>2</sub> content.

14 mol% exhibit, during the bending test, inelastic behaviour before failure, while compositions above 14 mol% behave elastically.

A different behaviour can be noted when hardness is tested; again there are increasing values with ceria addition, but in this case the maximum value corresponds to 32 mol% CeO<sub>2</sub>, as can be seen in Fig. 5.

The indentation morphologies are also quite different: there is no evidence of significant radial cracking until the CeO<sub>2</sub> content exceeds 24 mol%; but at higher ceria levels cracks begin to develop, as typically observed in most ceramic materials. Moreover, for low CeO<sub>2</sub> contents there is a limited amount of very localised fracture immediately adjacent to the indentation edges, mainly running parallel to the edges (Fig. 6); there is a region of surface uplift with granular appearance (Fig. 7)

which is not detectable for compositions above 24 mol%.

In the region where the maximum hardness develops both TZ<sup>0</sup> and TZ' are present. Therefore, when TZ<sup>0</sup> is replaced by TZ' phase, the material loses its plasticity and increases its hardness. It is possible to correlate the hardness trend in terms of bond energy of the phases present. Vickers hardness data expressed as GPa can be represented as volumetric energy data (GJ/m<sup>3</sup>) which can be qualitatively compared with the volumetric molar energies of thermodynamic origin. Molar lattice energies (*U*) were calculated as described by Evans,<sup>13</sup> and molar volumes were calculated by dividing the molecular weight by the XRD density. Finally, volumetric lattice energies (*E<sub>v</sub>*) were obtained by dividing the molar lattice energy of any composition (*U*) by its molar volume (*V*) following the Plendl-Gielisse approach.<sup>14</sup> Compositions and hardness values are reported in Table 2.

It can be easily seen that the Plendl-Gielisse approach provides a linear relationship between 'hardness', expressed as (*E<sub>v</sub>*) values and composition, whereas the measured data (*H<sub>v</sub>*) show a remarkable deviation from linearity in the first half of the diagram in the low ceria region. Beyond 50 mol% ceria there is fair linearity, quite comparable with the theoretical one.

In explaining this behaviour it is reasonable to expect low hardness values in 10–16 mol% ceria which belong to the group of materials in which transformation plasticity phenomena have been recorded.<sup>2,7,15,16</sup> In the low ceria solid solutions toughness increases have been explained via an

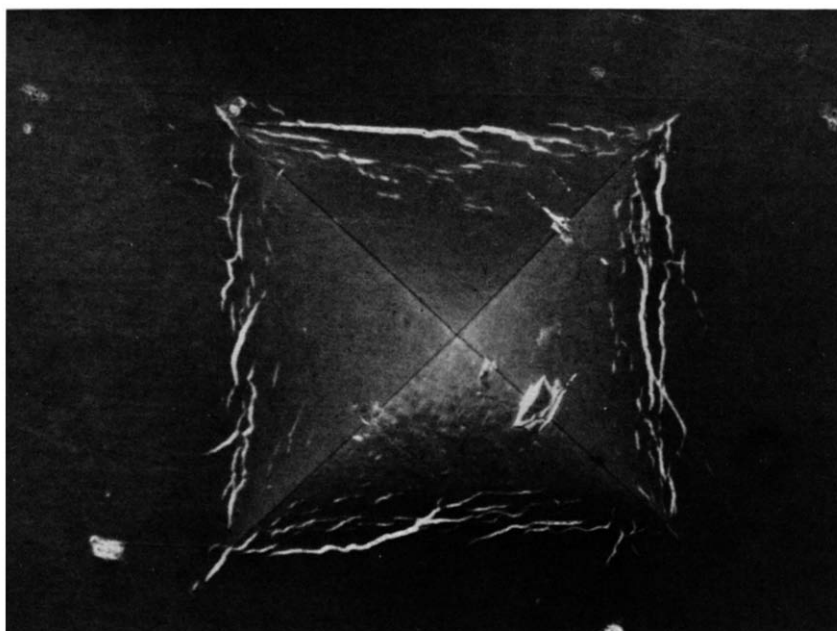


Fig. 6. SEM microstructure of a Vickers indentation (200 N) on a ZrO<sub>2</sub>-CeO<sub>2</sub> 12 mol% sample.

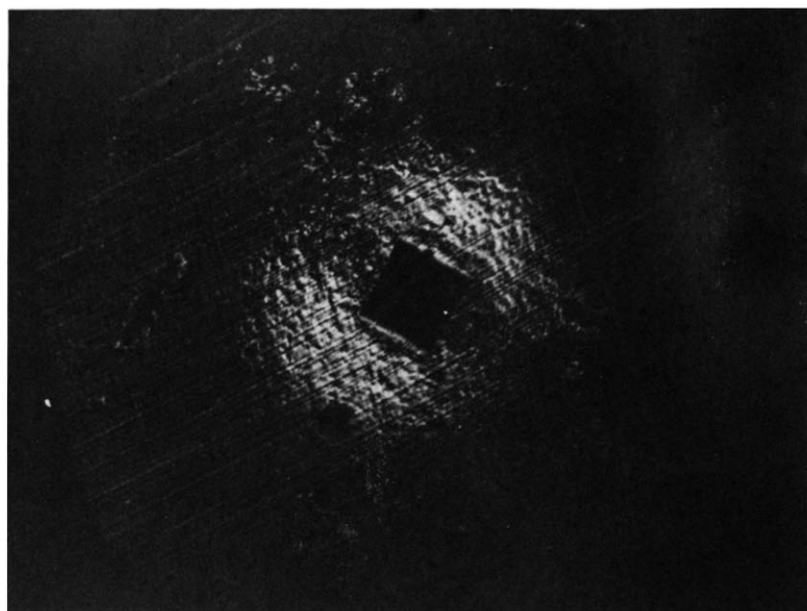


Fig. 7. Optical image (Nomarsky mode) of a Vickers indentation on a  $\text{ZrO}_2\text{-CeO}_2$  16 mol% sample.

extended  $t$ - $m$  transformation volume susceptible to large deformations under the plastic regime.

On the other hand, materials in the 24–48 mol% ceria range show higher hardness values because they contain  $\text{TZ}^0$  with increasing amounts of the so-called non-transformable  $\text{TZ}'$  phase, which is not prone to absorb the input energy of the indenter. The appearance of cracking and the loss of significant uplift correlate with the absence of any effective phase transformation due to the high imposed local indentation stresses, such that materials with  $\text{CeO}_2$  higher than 40 mol% are behaving in a normal brittle ceramic fashion.

Table 2. Lattice energies, molar volumes, volumetric lattice energies and Vickers hardness for the tested samples

$\text{CeO}_2$ (mol%)	$U$ (kJ/mol)	$V$ ( $\text{cm}^3/\text{mol}$ )	$E_v$ (kJ/ $\text{cm}^3$ )	$H_v$ (GPa)
0	11 195	20.49	546	<sup>a</sup>
10	11 180	20.66	540	6.3
12	11 175	20.77	538	6.3
14	11 150	20.82	535	6.3
16	11 134	20.87	533	6.5
24	11 050	21.18	522	7.5
32	10 929	21.48	509	8.0
40	10 851	21.90	496	7.6
48	10 774	22.29	489	7.5
60	10 656	22.47	474	5.5
70	10 543	22.93	460	5.2
80	10 434	23.35	447	4.8
90	10 326	23.76	435	4.1
100	10 255	24.15	425	3.9

<sup>a</sup> In the case of monoclinic zirconia mechanical properties were not tested.

#### 4 Conclusions

Studies have been carried out to investigate the mechanical properties, at room temperature, of samples ranging through the whole  $\text{ZrO}_2\text{-CeO}_2$  system.

Strength as well as toughness is at its highest in the presence of the transformable ( $\text{TZ}^0$ ) tetragonal phase. Further ceria addition degrades both properties, at first rapidly in the range where both the  $\text{TZ}^0$  and the non-transformable  $\text{TZ}'$  are stable then more slowly.

Hardness data have been correlated with bond energies and it has been shown that the 'thermodynamic hardness' concept of the volumetric energy ( $E_v$ ) is a viable approach in the case of the single, cubic phase materials.

#### Acknowledgements

This work has been financially supported by the Italian CNR (National Research Council)-PNF Special Materials for Advances Technologies-Structural Ceramics/Composites and the Ministry of Public Education.

#### References

1. Matsumoto, R. L. K., Aging behavior of Ce-stabilized tetragonal zirconia polycrystals. *J. Amer. Ceram. Soc.*, **71**(3) (1978) C128–9.

2. Tsukuma, K. & Shimada, M., Strength, fracture toughness and Vickers hardness of CeO<sub>2</sub>-stabilized tetragonal ZrO<sub>2</sub> polycrystals. *J. Mater. Sci.*, **20** (1985) 1178.
3. Meriani, S., A new single-phase tetragonal CeO<sub>2</sub>-ZrO<sub>2</sub> solid solution. *Mater. Sci. Engng.*, **71** (1985) 369.
4. Meriani, S. & Spinolo, G., Powder data for metastable Zr<sub>x</sub>Ce<sub>1-x</sub>O<sub>2</sub> ( $x=0.84$  to  $0.40$ ) solid solutions with tetragonal symmetry. *Powd. Diffr.*, **2**(4) (1987) 225.
5. Sato, T. & Shimada, M., Transformation of ceria-doped tetragonal zirconia polycrystals by annealing in water. *Amer. Ceram. Soc. Bull.*, **64**(10) (1985) 1382-4.
6. Tsukuma, K., Mechanical properties and thermal stability of CeO<sub>2</sub> containing tetragonal zirconia polycrystals. *Amer. Ceram. Soc. Bull.*, **65**(10) (1986) 1386-9.
7. Reyes-Morel, P. E., Cherng, J. S. & Chen, I., Transformation plasticity of CeO<sub>2</sub>-stabilized tetragonal zirconia polycrystals. II: Pseudoelasticity and shape memory effect. *J. Amer. Ceram. Soc.*, **71**(8) (1989) 648-57.
8. Heussner, K. H. & Claussen, N., Strengthening of ceria-doped tetragonal zirconia polycrystals by reduction-induced phase transformation. *J. Amer. Ceram. Soc.*, **72**(6) (1989) 1044-6.
9. Anstis, G. R., Chantikul, P., Lawn, B. R. & Marshall, D. B., A critical evaluation of indentation techniques for measuring fracture toughness. I: Direct crack measurements. *J. Amer. Ceram. Soc.*, **64**(9) (1981) 533-8.
10. Swain, M. V. & Claussen, N., Comparison of  $K_{Ic}$  values for Al<sub>2</sub>O<sub>3</sub>-ZrO<sub>2</sub> composites obtained from notch-beam and indentation strength techniques. *J. Amer. Ceram. Soc.*, **66**(2) (1983) C27-9.
11. Matsumoto, R. L. K., Evaluation of fracture toughness determination methods as applied to ceria-stabilised tetragonal zirconia polycrystals. *J. Amer. Ceram. Soc.*, **70**(12) (1987) C366-8.
12. Tani, E., Yoshimura, M. & Somiya, S., Revised phase diagram of the system ZrO<sub>2</sub>-CeO<sub>2</sub> below 1400°C. *J. Amer. Ceram. Soc.*, **66**(7) (1983) 506-10.
13. Evans, R. C., *An Introduction to Xtal Chem* (1st edn), 1948, pp. 21-3.
14. Plendl, J. N. & Gielisse, P. G., Hardness of non-metallic solids on an atomic basis. *Phys. Rev.*, **125**(3) (1962) 828-32.
15. Coyle, T. W., Coblenz, W. S. & Bender, B. A., Transformation toughening in large-grain-size CeO<sub>2</sub>-doped ZrO<sub>2</sub> polycrystals. *J. Amer. Ceram. Soc. Com.*, **71**(2) (1988) C88-92.
16. Schmid, C., Sbaizero, O. & Meriani, S., Shape-memory-like effect phenomena in a Ce-TZP/Al<sub>2</sub>O<sub>3</sub> composite. Submitted to the *J. Amer. Ceram. Soc. Com.*